Low-energy excitations in impurity substituted $CuGeO_3$

B. R. Jones, A. B. Sushkov, and J. L. Musfeldt
Department of Chemistry, State University of New York at Binghamton, Binghamton, New York 13902–6016

Y. J. Wang
National High Magnetic Field Laboratory, Florida State University, Tallahassee, Florida 32306

A. Revcolevschi and G. Dhalenne
Laboratoire de Physicochimie des Solides, Université Paris–Sud, 91405 Orsay Cédex, France
(Received 15 February 2000; revised manuscript received 5 September 2000; published 6 March 2001)

We report far-infrared reflectance measurements of Zn- and Si-doped $CuGeO_3$ single crystals as a function of applied magnetic field at low temperature. Overall, the low-energy far-infrared spectra are extraordinarily sensitive to the various phase boundaries in the *H-T* diagram, with the features being especially rich in the low-temperature dimerized state. Zn impurity substitution rapidly collapses the 44 cm^{-1} zone-boundary spin Peierls gap, although broadened magnetic excitations are observed at the lightest doping level (0.2%) and a remnant is still observable at 0.7% substitution. In a 0.7% Si-doped sample, there is no evidence of the spin gap. Impurity substitution effects on the intensity of the 98 cm^{-1} zone-folding mode are striking as well. The lightly doped Zn crystals display an enhanced response, and even at intermediate doping levels, the mode intensity is larger than that in the pristine material. The Si-doped sample also displays an increased intensity of the 98 cm^{-1} mode in the spin Peierls phase relative to the pure material. The observed trends are discussed in terms of the effect of disorder on the spin gap and 98 cm^{-1} mode, local oscillator strength sum rules, and broken selection rules.

DOI: 10.1103/PhysRevB.63.134414 PACS number(s): 75.30.Kz, 75.30.Hx, 78.30.−j

I. INTRODUCTION

Recently, there has been a great deal of interest in low-energy excitations of broken spin chains. This interest has been exemplified by theoretical work on the magnetic excitations of the broken chain, quantum phonons, the nature of the critical coupling, and the role of disorder.[1–10] Combined with the discovery of facile doping without severe structural modification in $CuGeO_3$,[11] which created enormous chemical tuning possibilities in the first inorganic spin Peierls (SP) system, there exists an experimental proving ground for interrupted spin chain systems as well as a theoretical basis from which to understand the results. This serendipity has moved the study of interrupted magnetic systems to a central place in solid state chemistry and physics.

$CuGeO_3$ is the first inorganic spin Peierls system; as such, the initial report by Hase, Terasaki, and Uchinokura generated a lot of activity.[12–14] In this compound, the low-dimensional spin system is comprised of localized Cu $S=1/2$ electrons, and the value of $J_\perp$ is fully 10% of $J_\parallel$ leading to many interesting effects. Zone center and boundary spin gaps have been identified at 17 and 44 cm^{-1}, respectively.[15,16] At the same time, neutron scattering studies have highlighted the complex behavior of the magnetic soliton in the high-field, incommensurate phase of pristine $CuGeO_3$.[17] Recent work has demonstrated the facile and interesting impurity substitution possibilities in $CuGeO_3$.[11,18] In the case of Zn doping, the impurity species is nonmagnetic, and is substituted for the d^9 Cu atoms in the octahedral lattice. Thus, systems with the formula $Cu_{1-x}Zn_xGeO_3$ can be prepared and provide an ideal model to study ''spin interruptions'' in a linear magnetic chain system. In contrast, Si replaces Ge to yield $CuGe_{1-y}Si_yO_3$, which primarily affects interchain coupling. One of the most attractive aspects of these doped compounds is that the cationic substitution takes place without severe modification of the linear chain structure.[11,19]

The competing ground states of impurity substituted $CuGeO_3$ have attracted a great deal of attention. With increasing Zn concentration, the SP transition temperature decreases and levels off near 9 K and is present up to $\approx 3\%$ doping when probed by susceptibility and has been detected at impurities levels of up to 8% via more local techniques.[20–23] Further, a three-dimensional (3D) antiferromagnetic (AF) Néel state is stabilized at lower temperature,[20,21,24–26] which competes with the SP phase and seems to need no critical concentration for its appearance. The neutron scattering investigations by Regnault *et al.* and Martin *et al.* on $Cu_{1-x}Zn_xGeO_3$ were particularly important for confirming the coexistence of SP and AF ordering.[27,28] This coexistence of coherent AF long range order and SP dimerization is predicted to persist even if the distribution of impurities along the chain is random.[29] X-ray scattering studies extended the aforementioned neutron scattering work on Zn and Ni substituted samples into the high-field incommensurate phase:[30] at low doping concentrations, a short-range ordered incommensurate phase is stabilized, attributed to strong pinning of the spin solitons to impurities.[31,32] At higher doping levels, long-range order is in competition with the SP phase. With Si doping, the SP temperature decreases slightly and 3D AF order sets in at lower temperature.[27,33] In fact, the SP phase coexists with the AF phase in this compound too, and a magnetic phase is present above 8 T. For the magnetic field aligned along the chain axis, a spin-flop phase is also observed.[34] Neutron scattering studies on Si substituted crystals has been pursued as well, most recently

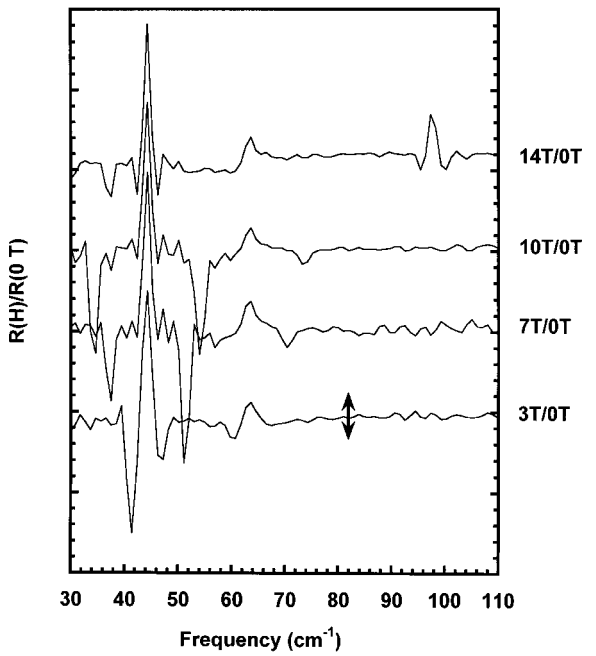

FIG. 1. Far-infrared reflectance ratios of $CuGeO_3$ as a function of applied magnetic field at 4.2 K. From bottom to top: 3 T/0 T, 7 T/0 T, 10 T/0 T, and 14 T/0 T. The curves have been offset for clarity. The arrow represents a 6% deviation from unity.

in high magnetic fields.[35] A variety of techniques have been used to map out *H-T* phase diagrams for Zn- and Si-doped crystals of particular concentrations.[34,36–38] The detailed structure of the most appropriate phase diagrams will be discussed later.

Several ESR measurements have focussed on the low-energy excitations in Zn and Si doped systems.[39–42] The multifrequency high-field spectra of Hassan *et al.* show particularly rich results, with a number of concentration dependent doping-induced features.[41] These effects are attributed to local enhancement of AF correlations near the Zn impurities, which give rise to transitions between states inside the SP gap. These results are in-line with predictions for in-gap states in doped $CuGeO_3$ by Martins *et al.*[9] Nojiri *et al.* show that minute Si doping significantly broadens the singlet-triplet absorption excitation due to spectral weight shift away from the triplet branch to the AF resonance mode.[42]

Far-infrared reflectance and transmission measurements have been used to explore the characteristics of the *H-T* phase diagram of $CuGeO_3$.[43–49] In the pristine material, weak folded modes are observed at 98, 284, 312, and 800 cm^{-1} below T_c.[44,45,49] The 98 cm^{-1} zone boundary mode (of B_{3u} symmetry) is polarized along the *a* axis.[49] Data through the dimerized $\rightarrow$ incommensurate transition are particularly striking.[47,48] Here, Zeeman splitting of the 44 cm^{-1} SP gap is observed; the lower and upper branches in the normalized spectra disappear in the incommensurate phase due to destruction of the singlet ground state. Takehana *et al.* also pointed out the broad absorption centered near 63 cm^{-1}, which is assigned as a magnetic excitation from the singlet ground state to a continuum state.[49]

Low-energy excitations in doped $CuGeO_3$ have also been studied previously by far-infrared spectroscopy. McGuire *et al.* observe several very low-frequency absorption lines with progressive Zn doping (10 and 20 cm^{-1}) as well as a broader temperature independent absorption.[50] The 10 cm^{-1} feature, assigned as a librational motion of the GeO_4 tetrahedra, is absent in Si-doped samples. The temperature dependence of the 20 cm^{-1} structure is consistent with a three-level model, in which the two excited states are slightly above the energy of the ground state. In Si- and Mg-doped $CuGeO_3$, Damascelli *et al.* observed a change in the 800 cm^{-1} *b*-polarized B_{2u} zone-boundary phonon mode on passing through the SP transition.[51] Integrated intensities as a function of temperature show a decrease in the transition temperature, a broadening of the transition regime, and a reduction of the order-parameter intensity compared to the undoped crystal. Surprisingly, the spectra of Zn-doped $CuGeO_3$ revealed no field dependence for the 10 and 20 cm^{-1} features.[50] Considering the richness of the pristine material, extension of earlier experiments by McGuire *et al.* to higher energy (above 30 cm^{-1}) is important.

In order to provide further information on the nature of the SP transition and the lattice dynamics of the underlying phases, we have investigated the infrared reflectance of several Zn- and Si-doped $CuGeO_3$ crystals as a function of applied magnetic field. Our goal is to identify the low-energy excitations which are important in these systems, determine the effect of doping, and more clearly understand the field effects in the low-temperature phases.

II. EXPERIMENTAL

Large, regularly shaped single crystals of doped $CuGeO_3$ were grown by floating zone techniques using an image furnace.[52] Doping levels of 0.2, 0.7, 1.5, and 4.0 % Zn and 0.7% Si were incorporated and were assessed by ICP/AES. The samples used for these experiments were cleaved from the originals along the *bc* plane. Typical dimensions were $\approx 0.4 \times 0.2 \times 0.3$ cm.

Unpolarized infrared reflectance measurements were performed at the National High Magnetic Field Laboratory (NHMFL) in Tallahassee, FL using a Bruker 113V Fourier transform infrared spectrometer.[53] Our runs were made using the 12, 23, and 50 μm Mylar beamsplitters, covering the frequency range from 30–200 cm^{-1}. A 20 T superconducting magnet was employed for the magnetic field work.[54] Using the applied field (and occasionally temperature) as adjustable tuning parameters, we were able to explore the previously determined phase diagrams of the various similarly doped samples, taking spectra in a new frequency region (complementary to that of McGuire *et al.*[50]) within several representative phases. A detailed description of the experimental setup at the National High Magnetic Field Laboratory is given elsewhere.[55]

These measurements were performed using the infrared reflectance probe developed at the NHMFL; a gold mirror was available as a reference. In this configuration, the incident light is 15° from normal to the sample surface, which is analogous to the canting procedure described by Takehana *et al.*[49] Thus, we are inherently sampling some *a*-axis contribution, although the majority of the response is from the *bc*

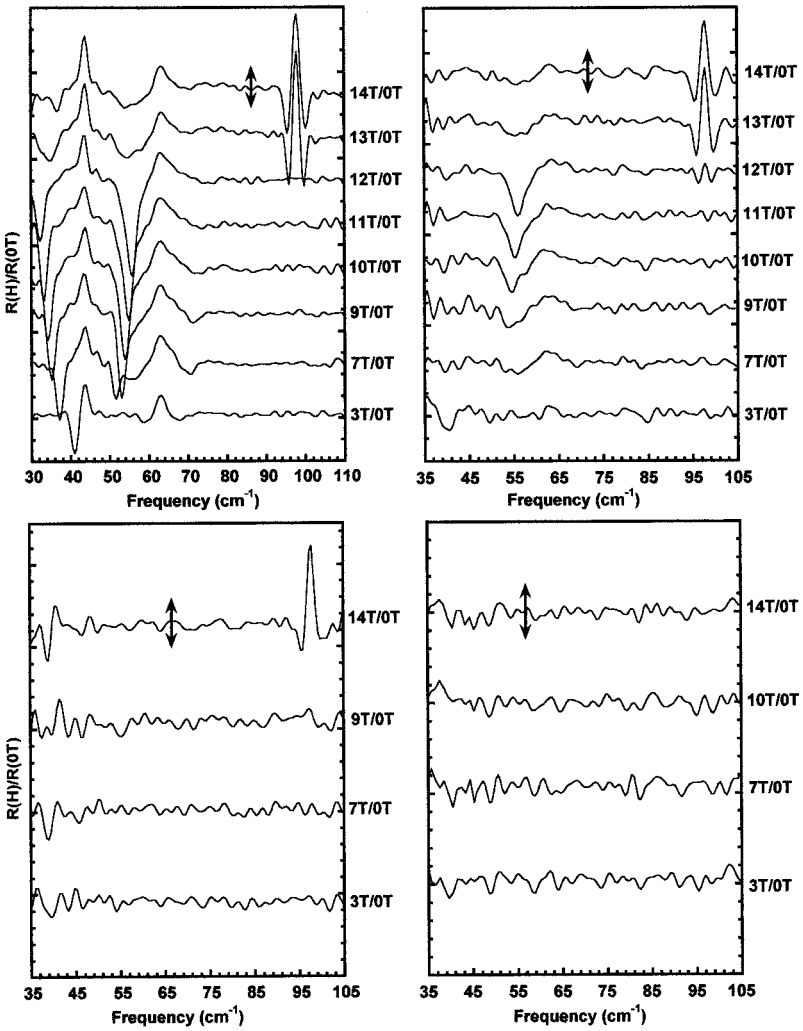

FIG. 2. Upper left panel: Far-infrared reflectance ratios of $Cu_{0.998}Zn_{0.002}GeO_3$ as a function of applied magnetic field at 4.2 K. The arrow represents a 10% deviation from unity. Upper right panel: Far-infrared reflectance ratios of $Cu_{0.993}Zn_{0.007}GeO_3$ as a function of applied magnetic field at 4.2 K. The arrow represents a 10% deviation from unity. Lower left panel: Far-infrared reflectance ratios of $Cu_{0.985}Zn_{0.015}GeO_3$ as a function of applied magnetic field at 4.2 K. The arrow represents a 6% deviation from unity. Lower right panel: Far infrared reflectance ratios of $Cu_{0.96}Zn_{0.04}GeO_3$ as a function of applied magnetic field at 4.2 K. The arrow represents a 6% deviation from unity. The curves have been offset for clarity in each case.

plane. In order to track changes with the applied field, we calculated reflectance ratios $\Delta R = R(H)/R(H=0)$. Here, both $R(H)$ and $R(H=0)$ are single beam spectra taken in an applied field and zero field, respectively. Because we are mainly concerned with field effects, both $R(H)$ and $R(H=0)$ are taken at 4.2 K to eliminate any temperature effects. The temperature dependence of pristine $CuGeO_3$ in the frequency range of interest here has been studied elsewhere.[49] The reflectance ratio provides a normalized reflectance response. Thus, deviations from unity are the important signal, and changes in the reflectance can be characterized with good accuracy. Typical noise variations are on the order of 2–3 % in this frequency range.

III. RESULTS

A. Undoped $CuGeO_3$

Figure 1 displays the far-infrared reflectance ratio spectra of undoped $CuGeO_3$ as a function of magnetic field. The well-known Zeeman splitting of the zone boundary SP gap is very pronounced at low fields; disappearance of this structure above the 12.5 T critical field is attributed to destruction of the singlet ground state above the dimerized → incommensurate phase boundary.[47,48] The zone center gap is observed at 17 cm^{-1}.[15,16] Initial observation and excitement about these low-frequency structures prevented notice of two smaller features near 63 and 98 cm^{-1}. These modes have recently been attributed to a *b*-polarized excitation from the singlet state to the magnetic continuum and an *a*-polarized zone folding phonon mode of B_{3u} symmetry, respectively.[49] Note that the 98 cm^{-1} reflectance ratio peak is indicative of a mode in the SP phase; that it appears as a peak in the high field reflectance ratio (Fig. 1) is due to absorption in the denominator.[56] That the 98 cm^{-1} feature in $CuGeO_3$ is characteristic of the SP phase was observed previously by Takehana *et al.*; it displays doublet structure in the incommensurate phase that is related to the degree of incommensurability.[49] This doublet structure is manifested in the high field reflectance ratio spectrum as two lobes on either side of the 98 cm^{-1} feature.

B. Zn-doped $CuGeO_3$

1. Lightest Zn doping: $Cu_{0.998}Zn_{0.002}GeO_3$

The upper left-hand panel of Fig. 2 displays the reflectance ratio of 0.2% Zn substituted $CuGeO_3$ at different applied fields. Although the low-energy magnetic excitations are similar to those in the pristine material, they are broader and less well defined. Despite this broadening, the magnitude

of the Zeeman splitting is the same as that in Fig. 1. Note that the upper branch of the Zeeman splitting saturates near 55 cm^{-1} in the reflectance ratio.

In the lightest Zn-doped sample, the 98 cm^{-1} feature appears with strong intensity and a fairly unusual line shape above the SP $\rightarrow$ incommensurate phase boundary.[57] This structure is much more pronounced than that in pristine $CuGeO_3$. Based on the well-known result from a number of experiments that doping weakens the lattice distortion and destabilizes the SP phase, this result was unexpected.[45]

2. Light Zn doping: $Cu_{0.993}Zn_{0.007}GeO_3$

Light Zn doping (0.7%) of $CuGeO_3$ results in overall modest changes to the *H-T* phase diagram.[36] Essentially, the area of the SP phase is smaller due to a reduced transition temperature and critical field. This is because the long-range ordered phase (driven by electron-electron interactions) is gaining ground compared to the magnetoelastically stabilized phase. No new phase boundaries in *H-T* space have been identified at this doping level.

Despite the similar *H-T* phase diagram to that of the pristine $CuGeO_3$ system, the reflectance ratio spectra of the 0.7% Zn doped sample, shown in the upper right-hand panel of Fig. 2, display a dramatically different response. The reflectance ratio in the SP phase develops a broad structure near 55 cm^{-1} with increasing field; it becomes fairly pronounced ($\approx$13% deviation from unity) upon approach to H_c. This structure is assigned as a remnant of the SP gap, with likely contributions from the upper branch of the Zeeman splitting and the 63 cm^{-1} singlet$\rightarrow$continuum excitation, superimposed upon one another.[58] This composite structure shifts weakly to higher frequency with applied field in the SP phase.[59] The 55 cm^{-1} feature is sensitive to the 12 T phase boundary as well; only a residual signature persists up to 17 T.

In the lightly doped Zn sample (0.7%), the 98 cm^{-1} feature again appears with enhanced intensity relative to the pristine material, although it is considerably damped compared to that of $Cu_{0.998}Zn_{0.002}GeO_3$. This observation as well as the changing line shape will be discussed in detail later.

3. Intermediate Zn doping: $Cu_{0.985}Zn_{0.015}GeO_3$

Increased doping complicates the *H-T* phase diagram of the $CuGeO_3$ system. With 1.5% Zn doping, both SP and AF states are stabilized at low temperatures; a spin flop phase is also observed with $H \| c$.[36] Coexistence of the SP and AF phases is substantial near 4 K, with the AF contribution trailing off above 5 K.[27–29] A magnetic phase is stabilized above the 9.5 T critical field, and the incommensurate $\rightarrow$ uniform phase boundary has a different slope.

The lower left-hand panel of Fig. 2 displays the far-infrared reflectance ratios of $Cu_{0.985}Zn_{0.015}GeO_3$ taken at 4.2 K in different magnetic fields. No systematic low-energy reflectance ratio features develop with applied field below H_c. This is because the material is dirty and the gap has closed. The dimerized $\rightarrow$ incommensurate phase boundary is characterized by the appearance of the 98 cm^{-1} feature; it is less intense than in the 0.2 and 0.7 % Zn substituted samples but still stronger than that in the pristine material. Note that the progressive Zn doping has not affected the resonance frequency of this structure, although the shape has changed slightly. The negative lobes around the 98 cm^{-1} reflectance ratio peak weaken with greater impurity incorporation.

4. Heavy doping: $Cu_{0.96}Zn_{0.04}GeO_3$

With heavy Zn doping, the *H-T* phase diagram is modified yet again.[36] The SP transition itself becomes extremely weak, and in certain physical measurements (such as susceptibility) it is difficult to detect, although more local probes (such as neutron scattering) can still find the transition signature.[20,21,24–26] Pretransitional elastic fluctuations in heavily doped $CuGeO_3$ samples indicate some SP aspect to the low-temperature state, although AF interactions are important too.[36]

Far-infrared reflectance ratio spectra of the 4.0% doped $CuGeO_3$ sample are shown in the lower right-hand panel of Fig. 2. At 4.2 K, the in-field spectra follow a path along a phase boundary line where both SP and AF phases coexist. No low-energy excitations are observed in the energy regime of the spin gap. In independent runs, the intensity of the 98 cm^{-1} mode was variable, ranging from 0$\rightarrow$1.8% deviation from unity upon entry into the high-field phase. This variability (and the overall weak response) is reflected in the data of Fig. 4 (main panel and inset). Preliminary far-infrared reflectance ratio results at 6.5 K (not shown), which is further away from the AF/SP boundary, indicate that the heavily doped Zn sample is devoid of field-induced structure under these conditions as well.

C. Si-doped $CuGeO_3$

Whereas Zn doping replaces copper sites in the $CuGeO_3$ lattice, Si doping replaces Ge sites: a 0.7% doped sample will have the formula $CuGe_{0.993}Si_{0.007}O_3$. Thus, the main effect of Si doping is to modulate the interchain interactions via the introduction of distorted tetrahedons.[60] Although details of the *H-T* diagram seem to be sensitive to the nature of the probe, the general characteristics are clear.[34,37] There is a lowered zero-field transition temperature, below which both a SP phase and an AF/SP coexistence lie. A magnetic phase is observed above 8 T; the slope between the incommensurate and uniform phases is positive.

Reflectance ratio spectra of the 0.7% Si-doped crystal are displayed in Fig. 3. Within the SP phase, the far infrared reflectance ratios do not show any field dependent features. Light Si doping (Fig. 3) seems to be more effective than light Zn doping (Fig. 2) at ridding the system of low-energy magnetic excitations. Transition to the high field phase is marked by the appearance of the 98 cm^{-1} feature with moderate intensity; note that it is larger than in the pristine material. As in the previous data, the 98 cm^{-1} mode appears as a peak due to absorption in the denominator. This is because the zone-folding mode is a characteristic of the SP phase.

IV. DISCUSSION

A. Low-energy regime

Excitations of magnetic origin are anticipated in the low-energy regime, and these spin excitations are expected to be very local. Theoretical work by Martins *et al.* predicts the

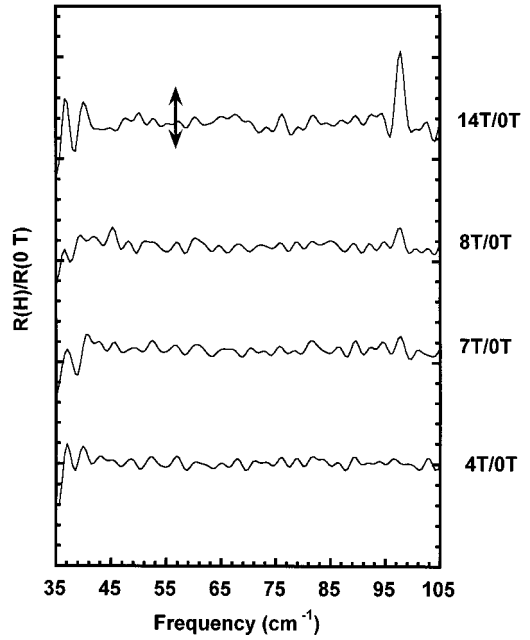

FIG. 3. Far-infrared reflectance ratios of $CuGe_{0.993}Si_{0.007}O_3$ as a function of applied magnetic field at 4.2 K. From bottom to top: 4 T/0 T, 7 T/0 T, 8 T/0 T, and 14 T/0 T. The arrow represents a 6% deviation from unity. The curves have been offset for clarity.

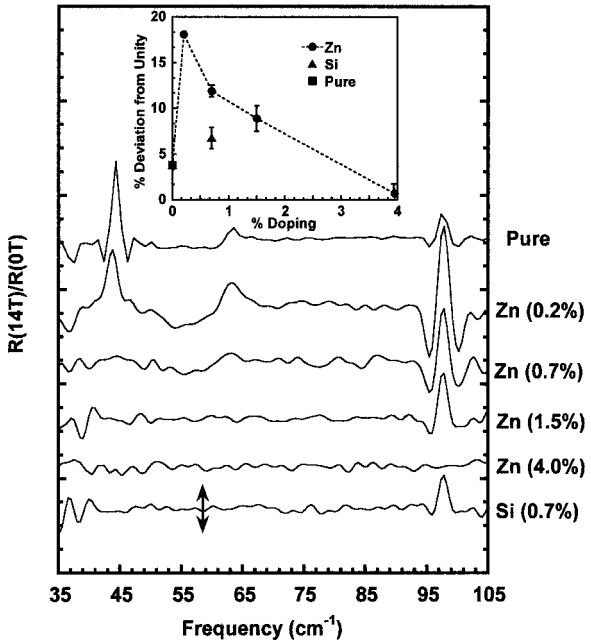

FIG. 4. 14 T/0 T reflectance ratios of $CuGeO_3$-based single crystals at different doping levels. From top to bottom: pure $CuGeO_3$, 0.2% Zn doped sample, 0.7% Zn doped sample, 1.5% Zn doped sample, 4.0% Zn doped sample, and 0.7% Si doped sample. The arrow represents a 10% deviation from unity. The curves have been offset for clarity. Inset: Deviation from unity of 98 cm^{-1} feature in the 14 T/0 T reflectance ratio spectra of doped $CuGeO_3$ samples as a function of dopant concentration. Error bars were determined using data from multiple runs.

rapid suppression of the spin gap in $CuGeO_3$ with Zn doping and the appearance of a number of in-gap states due to the breaking of spin singlets with in-chain substitution.[9,61] With decreasing dimerization (increased doping), the spectral weight inside the gap changes due to free spin coupling and singlet/triplet excitation effects. Enhanced AF correlations are predicted to occur near the spin vacancies. At very high doping levels, the gap will close. This model addresses energy scales near and below the gap, but in order for it to apply, there must be some remnant of the SP state in the material. From the data in Figs. 1 and 2, Zn doping at higher levels (1.5 and 4.0 %) produces substantial damage to the spin chain. The lack of structure in the far-infrared reflectance ratio of the medium and heavily doped samples near the 44 cm^{-1} spin gap suggests that the two lightly doped (0.2 and 0.7 % Zn) materials are the only possible candidates for interpretation within this model, as magnetic excitations in the other more heavily substituted crystals are eliminated by disorder.

Disorder broadens the magnetic excitations in the two lightly doped Zn samples (Fig. 2) compared to those of pure $CuGeO_3$ (Fig. 1). Nevertheless, the spin gap clearly survives the introduction of limited disorder. While wider, broader structures are observed in the case of 0.2% substitution, a more drastic effect is found for 0.7% Zn doping, indicating that the spin gap is substantially filled at this point. In fact, it seems likely that the 44 cm^{-1} spin gap and the 63 cm^{-1} singlet $\rightarrow$ continuum excitation in the pristine material combine and collapse to form the 55 cm^{-1} structure in $Cu_{0.993}Zn_{0.007}GeO_3$ (upper right-hand panel, Fig. 2).[62] The small frequency shift of the 55 cm^{-1} structure with applied field and its sensitivity to the SP $\rightarrow$ incommensurate phase boundary lends support to this hypothesis. Investigations on intermediate concentration samples to follow the detailed decay of the gap signature with doping are of interest in the future.[63–69] That similar Si doping (0.7%) causes a complete collapse of the SP gap is also curious, as it shows the stronger effects of interchain disruption on the spin gap. This result is in line with the ESR work of Nojiri *et al.*[42]

B. 98 cm^{-1} mode

Doping effects on the intensity of the 98 cm^{-1} mode are striking as well. Figure 4 displays 14 T/ 0 T reflectance ratio data for all samples investigated, and the inset summarizes the trend as a function of doping. The intensity of the 98 cm^{-1} mode first rises sharply, then gradually decreases with greater doping levels.

The observation of the 98 cm^{-1} mode in the dimerized phase of $CuGeO_3$ and the energy at which it appears motivated previous authors to classify this feature as an *a*-polarized folded phonon mode, which is an electric dipole-allowed transition resulting from the structural distortion.[49] Based upon the 98 cm^{-1} mode's behavior in the incommensurate phase, it is believed to be the folded phonon with the strong spin-phonon coupling, and therefore one of the modes contributing to the SP mechanism.[49] That this mode is strongly coupled to the spins might explain it's enhanced sensitivity to magnetic field in the doped samples.[14] It is well known, however, that increased doping stabilizes the AF phase (at the expense of the SP phase) in these materials,

thus decreasing the lattice distortion. A weaker lattice distortion should therefore translate into a less intense folded phonon mode[51]–a trend opposite to that in Fig. 4. Disorder-induced line broadening is expected as well.[70]

One possible resolution to this discrepancy is that light doping may preserve a local SP domain where the lattice distortion is quite strong, but further doping produces too much damage to preserve the dimerization in a meaningful way. Thus, a local probe (such as infrared spectroscopy) could detect such a short-range distortion, whereas a more long-range probe might not. Local enhancement effects were also argued in the interpretation of high-field ESR results, although here, it was the AF correlations that were of interest.[41] An alternative view is to assign the 98 cm^{-1} feature as an impurity-induced local phonon mode.[71] Such a feature has been identified in doped $CuGeO_3$ at 10 cm^{-1}.[50] That the 98 cm^{-1} mode grows with doping and seems to be associated with the spin Peierls distortion supports such an assignment, but the 98 cm^{-1} feature is observed in pristine $CuGeO_3$, making this description less satisfying. The most promising explanation for the trend in Fig. 4 preserves assignment of the 98 cm^{-1} feature as a zone-folded mode and accounts for effects from both a decrease in dimerization and a breakdown of selection rules due to impurity incorporation. As discussed previously, one expects the intensity of the 98 cm^{-1} folded phonon to decrease as the SP dimerization is destabilized with increased doping.[72] At the same time, defect incorporation may break the optical selection rules, allowing excitations in other polarizations or in other locations in the Brillouin zone.[73,74] That the 98 cm^{-1} mode is more intense in the doped samples suggests a breakdown of the selection rules caused by impurity incorporation and site symmetry reduction, therefore allowing this excitation in the bc plane. A superposition of these two effects might explain the observed trends in Fig. 4. With small levels of doping, the intensity of the 98 cm^{-1} mode increases due to the breakdown of selection rules. As the level of doping increases, the destabilization of the SP dimerization begins to dominate, and the intensity of the mode begins to drop. It is of future interest to see if field effects on the 800 cm^{-1} folded mode display similar trends. The temperature variation of the 800 cm^{-1} mode shows only normal lattice distortion effects.[51]

Finally, careful analysis of single beam spectra taken in the SP and incommensurate phases shows that while the 98 cm^{-1} feature is sharp and well-defined in the SP phase, it is broad, weak, and ill-defined (in frequency) in the incommensurate phase. Thus, passing from the dimerized to the incommensurate phase, the local oscillator strength is ''spread'' over a wider (≈ 8 cm^{-1}) frequency range. Conversely, passing from the incommensurate phase to the SP phase, the oscillator strength is ''squeezed'' into a small (≈ 2 cm^{-1}) region. Such a local sum rule is indicative of disorder, and in some ways analogous to the effect of magnetic impurities in dilute Kondo systems and to Zn doping in copper oxide superconductors.[75–77] The negative lobes in the 98 cm^{-1} reflectance ratio data of $Cu_{0.998}Zn_{0.002}GeO_3$, $Cu_{0.993}Zn_{0.007}GeO_3$, and $Cu_{0.985}Zn_{0.015}GeO_3$ (Fig. 4) are related to local oscillator strength changes between the dimerized and incommensurate phases,[78] and are identical to the doublet structure observed by Takehana *et al.* in the high field phase of pristine $CuGeO_3$. The splitting of this doublet structure is proportional to the degree of incommensurability.[49] From the data in Fig. 4, neither the absolute doping level nor intrachain-interchain substitution affects the position of these lobes. Using this measure, doping does not affect the degree of incommensurability in $CuGeO_3$ above H_c. Judging by the intensity of these structures, however, the incommensurability seems most stable at light doping levels.

V. CONCLUSION

In conclusion, we report far-infrared reflectance measurements on high-quality single crystal samples of both Zn and Si impurity substituted $CuGeO_3$ as a function of magnetic field in order to characterize the microscopic nature of the different low-temperature phases. Light doping is found to collapse the zone-boundary SP gap very quickly, although the spin gap does survive the introduction of limited disorder. At 0.2% Zn doping, the Zeeman splitting of the spin gap is broader and less well defined than that in the pristine material; at 0.7% Zn doping, only a remnant of the spin gap remains, centered near 55 cm^{-1}. Doping effects on the intensity of the zone-folding 98 cm^{-1} mode are also remarkable. The observed trends are discussed in terms of the effect of disorder on the spin gap and the 98 cm^{-1} mode.

ACKNOWLEDGMENTS

Financial support from the Materials Science Division, Basic Energy Sciences at the U.S. Department of Energy (Grant No. DE-FG0299ER45741) and the Division of Materials Research at the National Science Foundation (Grant No. DMR-9623221) is gratefully acknowledged. These measurements were performed at the National High Magnetic Field Laboratory in Tallahassee, FL, which is supported by NSF Cooperative Agreement No. DMR-9527035 and by the State of Florida. J.L.M. thanks the Visiting Scientist Program at the National High Magnetic Field Lab and the Dean's Research Semester Program at SUNY-Binghamton for the opportunity to pursue this project. We acknowledge stimulating discussions with G. L. Carr, E. Dagotto, C. C. Homes, and T. Timusk.

[1] G.S. Uhrig, Phys. Rev. Lett. **79**, 163 (1997).
[2] J. Riera and A. Dobry, Phys. Rev. B **51**, 16 098 (1995).
[3] G. Castilla, S. Chakravarty, and V.J. Emery, Phys. Rev. Lett. **75**, 1823 (1995).
[4] M. Azzouz and C. Bourbonnais, Phys. Rev. B **53**, 5090 (1996).
[5] J. Zang, A.R. Bishop, and D. Schmeltzer, Phys. Rev. B **52**, 6723 (1995).
[6] A.W. Sandvik, R.R.P. Singh, and D.K. Campbell, Phys. Rev. B

56, 14 510 (1997).
[7] A.W. Sandvik and D.K. Campbell, Phys. Rev. Lett. **83**, 195 (1999).
[8] R.J. Bursill, R.H. McKenzie, and C.J. Hamer, Phys. Rev. Lett. **83**, 408 (1999).
[9] G. Balster Martins, E. Dagotto, and J.A. Riera, Phys. Rev. B **54**, 16 032 (1996).
[10] M. Fabrizio, R. Mélin, and J. Souletie (unpublished).
[11] M. Hase, I. Terasaki, Y. Sasago, K. Uchinokura, and H. Obara, Phys. Rev. Lett. **71**, 4059 (1993).
[12] M. Hase, I. Terasaki, and K. Uchinokura, Phys. Rev. Lett. **70**, 3651 (1993).
[13] J.P. Boucher and L.P. Regnault, J. Phys. I **6**, 1939 (1996).
[14] J.L. Musfeldt (unpublished).
[15] M. Nishi, O. Fujita, and J. Akimitsu, Phys. Rev. B **50**, 6508 (1994).
[16] T.M. Brill, J.P. Boucher, J. Voiron, G. Dhalenne, A. Revcolevschi, and J.P. Renard, Phys. Rev. Lett. **73**, 1545 (1994).
[17] H.M. Rønnow, M. Enderle, D.F. McMorrow, L.-P. Regnault, G. Dhalenne, A. Revcolevschi, A. Hoser, K. Prokes, P. Vorderwisch, and H. Schneider, Phys. Rev. Lett. **84**, 4469 (2000).
[18] G. Dhalenne, A. Revcolevschi, J.C. Rouchaud, and M. Fedoroff, Mater. Res. Bull. **32**, 939 (1997).
[19] At higher doping levels, there is a linear variation of the crystalographic parameters in the Si-doped crystal (Ref. 60).
[20] Y. Sasago, N. Koide, K. Uchinokura, M.C. Martin, M. Hase, K. Hirota, and G. Shirane, Phys. Rev. B **54**, R6835 (1996).
[21] B. Grenier, J.-P. Renard, P. Veillet, C. Paulsen, G. Dhalenne, and A. Revcolevschi, Phys. Rev. B **58**, 8202 (1998).
[22] In contrast, the disappearance of the SP transition above a critical dopant concentration in $Cu_{1-x}Mg_xGeO_3$ is ascribed to a drastically reduced SP coherence length above a critical concentration driven by interchain interactions (Ref. 23).
[23] Y.J. Wang, V. Kiryukhin, R.J. Birgeneau, T. Masuda, I. Tsukada, and K. Uchinokura, Phys. Rev. Lett. **83**, 1676 (1999).
[24] R. Kadono, J. Phys. Soc. Jpn. **66**, 505 (1997).
[25] K.M. Kojima, Y. Fudamoto, M. Larkin, G.M. Luke, J. Merrin, B. Nachumi, Y.J. Uemura, M. Hase, Y. Sasago, K. Uchinokura, Y. Ajiro, A. Revcolevschi, and J.-P. Renard, Phys. Rev. Lett. **79**, 503 (1997).
[26] B. Büchner, T. Lorenz, R. Walter, H. Kierspel, A. Revcolevschi, and G. Dhalenne, Phys. Rev. B **59**, 6886 (1999).
[27] L.P. Regnault, J.P. Renard, G. Dhalenne, and A. Revcolevschi, Europhys. Lett. **32**, 579 (1995).
[28] M.C. Martin, M. Hase, K. Hirota, G. Shirane, Y. Sasago, N. Koide, and K. Uchinokura, Phys. Rev. B **56**, 3173 (1997).
[29] H. Fukiyama, T. Tanimoto, and M. Saito, J. Phys. Soc. Jpn. **65**, 1182 (1996).
[30] V. Kiryukhin and B. Keimer, J.P. Hill, S.M. Coad, and D.McK. Paul, Phys. Rev. B **54**, 7269 (1996).
[31] The solitonic modulation provides an appropriate description of the spin excitations near the 14 T field boundary, but at higher field, the dimerization amplitude takes on a sinusoidal modulation. The development of one form from the other (solitonic $\rightarrow$sinusoidal) seems to be continuous (Ref. 32). High field nueron scattering results show that the soliton lattice has both magnetic and structural components, with a combination of staggered and uniform magnetizations, respectively. Two different length scales apply as well (Ref. 17).
[32] T. Lorenz, B. Büchner, P.H.M. van Loosdrecht, F. Schönfeld, G. Chouteau, A. Revcolevschi, and G. Dhalenne, Phys. Rev. Lett. **81**, 148 (1998).
[33] J.-P. Renard, K. Le Dang, P. Veillet, G. Dhalenne, A. Revcolevschi, and L.-P. Regnault, Europhys. Lett. **30**, 475 (1995).
[34] M. Poirier, R. Beaudry, M. Castonguay, M.L. Plummer, G. Quirion, F.S. Razavi, A. Revcolevschi, and G. Dhalenne, Phys. Rev. B **52**, R6971 (1995).
[35] B. Grenier, L.P. Regnault, J.E. Lorenzo, J. Voiron, J. Bossy, J.P. Renard, G. Dhalenne, and A. Revcolevschi, Europhys. Lett. **44**, 511 (1998).
[36] P. Fronzes, M. Poirier, A. Revcolevschi, and G. Dhalenne, Phys. Rev. B **55**, 8324 (1997).
[37] H. Nojiri, T. Hamamoto, Z.J. Wang, S. Mitsudo, M. Motokawa, S. Kimura, H. Ohta, A. Ogiwara, O. Fujita, and J. Akimitsu, J. Phys.: Condens. Matter **9**, 1331 (1997).
[38] T. Masuda, I. Tsukada, K. Uchinokura, Y.J. Wang, V. Kiryukhin, and R.J. Birgeneau, Phys. Rev. B **61**, 4103 (2000).
[39] M. Hase, K.M.S. Etheredge, S.J. Hwu, K. Hirota, and G. Shirane, Phys. Rev. B **56**, 3231 (1997).
[40] P. Fronzes, M. Poirier, A. Revcolevschi, and G. Dhalenne, Phys. Rev. B **56**, 7827 (1997).
[41] A.K. Hassan, L.A. Pardi, G.B. Martins, G. Cao, and L.-C. Brunel, Phys. Rev. Lett. **80**, 1984 (1998).
[42] H. Nojiri, H. Ohta, S. Okubo, W. Fujita, J. Akimitsu, and M. Motokawa, J. Phys. Soc. Jpn. **68**, 3417 (1999).
[43] Z.V. Popović, S.D. Devic, V.N. Popov, G. Dhalenne, and A. Revcolevschi, Phys. Rev. B **52**, 4185 (1995).
[44] M.N. Popova, A.B. Sushkov, S.A. Golubchik, A.N. Vasil'ev, and L.I. Leonyuk, Phys. Rev. B **57**, 5040 (1998).
[45] A. Damascelli, D. van der Marel, F. Parmigiani, G. Dhalenne, and A. Revcolevschi, Phys. Rev. B **56**, R11373 (1997).
[46] A. Damascelli, D. van der Marel, F. Parmigiani, G. Dhalenne, and A. Revcolevschi, Physica B **244**, 114 (1998).
[47] G. Li, J.L. Musfeldt, Y.J. Wang, S. Jandl, M. Poirier, A. Revcolevschi, and G. Dhalenne, Phys. Rev. B **54**, R15 633 (1996).
[48] P.H.M. van Loosdrecht, S. Huant, G. Martinez, G. Dhalenne, and A. Revcolevschi, Phys. Rev. B **54**, R3730 (1996).
[49] K. Takehana, T. Takamasu, M. Hase, G. Kido, and K. Uchinokura, Phys. Rev. B **62**, 5191 (2000).
[50] J.J. McGuire, T. Room, T.E. Mason, T. Timusk, H. Dabkowska, S.M. Coad, and D.McK. Paul, Phys. Rev. B **59**, 1157 (1999).
[51] A. Damascelli, D. van der Marel, G. Dhalenne, and A. Revcolevschi, Phys. Rev. B **61**, 12 063 (2000).
[52] A. Revcolevschi and R. Collongues, C. R. Acad. Bulg. Sci. **266**, 1767 (1969).
[53] Unfortunately, polarized measurements are not currently possible with this setup.
[54] The field was applied along the *a* crystallographic axis.
[55] H.K. Ng and Y.J. Wang, *Physical Phenomena at High Magnetic Fields II*, edited by Z. Fisk, L. Gor'kov, D. Meltzer, and R. Schrieffer (World Scientific, Singapore, 1995).
[56] We observe the *a* polarized 98 cm^{-1} structure in our spectra because of the 15° angle of the incident light in our configuration. Therefore, we are sampling some *a*-axis response, though the majority of the response is from the *bc* plane. This is analagous to the sample-canting procedure described by Takehana *et al.* (Ref. 49).
[57] Because the 63 and 98 cm^{-1} features are excitations of the SP

phase, the peak in the reflectance ratio is due to a dip in the denominator (not a maximum in the numerator).

[58] Within our sensitivity, we did not observe the lower branch of the Zeeman splitting between 30–35 cm^{-1} in the 0.7% doped sample.

[59] Careful examination of the reflectance ratio data suggests that a harmonic of the gap may exist at 88 cm^{-1}. Efforts to improve our experimental sensitivity are underway.

[60] M. Weiden, R. Hauptmann, W. Richter, C. Geibel, P. Hellmann, M. Köppen, F. Steglich, M. Fischer, P. Lemmens, G. Güntherodt, A. Krimmel, and G. Nieva, Phys. Rev. B **55**, 15 067 (1997).

[61] Simulations involving substitutions between chains are technically more difficult.

[62] This position corresponds to the upper branch of the Zeeman splitting.

[63] The lightly doped regime is also of great current interest in the manganites, nicklates, and cuprates (Ref. 64–69).

[64] S. Yunoki, J. Hu, A.L. Malvezzi, A. Moreo, N. Furukawa, and E. Dagotto, Phys. Rev. Lett. **80**, 845 (1998).

[65] A. Moreo, S. Yunoki, and E. Dagotto, Phys. Rev. Lett. **83**, 2773 (1999).

[66] E. Dagotto, J. Riera, A. Sandvik, and A. Moreo, Phys. Rev. Lett. **76**, 1731 (1996).

[67] K.R. Thurber, A.W. Hunt, T. Imai, F.C. Chou, and Y.S. Lee, Phys. Rev. Lett. **79**, 171 (1997).

[68] A.W. Hunt, P.M. Singer, K.R. Thurber, and T. Imai, Phys. Rev. Lett. **82**, 4300 (1999).

[69] C. Buhler, S. Yunoki, and A. Moreo, Phys. Rev. B **62**, R3620 (2000).

[70] A.M. Stoneham, Rev. Mod. Phys. **41**, 82 (1969).

[71] T. Timusk (private communication).

[72] Folded phonons in pure and doped $CuGeO_3$ with temperature display this order-parameter behavior (Ref. 51).

[73] F.A. Cotton, *Chemical Applications of Group Theory*, 2nd ed. (Wiley, New York, 1990).

[74] M.H. Brodsky and A. Lurio, Phys. Rev. B **9**, 1646 (1974).

[75] L. Degiorgi, Rev. Mod. Phys. **71**, 687 (1999).

[76] D.A. Bonn, S. Kamal, Kuan Zhang, Ruixing Liang, D.J. Baar, E. Klein, and W.N. Hardy, Phys. Rev. B **50**, 4051 (1994).

[77] D.N. Basov, A.V. Puchkov, R.A. Hughes, T. Strach, J. Preston, T. Timusk, D.A. Bonn, R. Liang, and W.N. Hardy, Phys. Rev. B **49**, 12 165 (1994).

[78] Note that these lobes are also weakly present in the pristine material.